A Highly Active Defect Engineering Cl-doped Carbon Catalyst for N_2 Reduction Reaction

Minxue Huang,[1#] Shipeng Gong,[1#] Sini Wang,[3] Kang Yang,[1] Shi Chen,[1] Changlai Wang,[1] Xiangkai Kong,[3*] and Qianwang Chen[1,2*]

[1]Hefei National Laboratory for Physical Science at Microscale and Department of Materials Science & Engineering, University of Science and Technology of China, Hefei 230026, China

[2]Anhui Province Key Laboratory of Condensed Matter Physics at Extreme Conditions, High Magnetic Field Laboratory of Chinese Academy of Sciences, Hefei 230031, China

[3]Key Laboratory of Green and Precise Synthetic Chemistry and Application, Ministry of Education & Anhui Province Key Laboratory of Pollutant Sensitive Materials and Environmental Remediation, Huaibei Normal University, Huaibei, Anhui 235000,China

[#] These authors contributed equally to this work.

[*]Correspondence to: cqw@ustc.edu.cn
kxk@chnu.edu.cn

Experimental Details

1. **Materials Preparation:** $Zn(CH_3COO)_2{\cdot}2H_2O$ (>99%), NaCl (>99.5%), KCl (>99.5%), $ZnCl_2$ (>98%), $LiCl{\cdot}H_2O$ (>97%) was purchased from Sinopharm Chemical Reagent Co. Ltd (AR grade, China). 1,3,5-Benzenetricarboxylic acid (99%) was purchased from J&K Chemical. Nafion solution (5 wt%) were purchased from Sigma-Aldrich. All reagents were directly used without further treatment.

   Preparation of Carbon nanorods (CR): 0.55 g $Zn(CH_3COO)_2{\cdot}2H_2O$ was dispersed in 10 ml aqueous solution to form solution A. 0.525 g of 1,3,5-benzenetricarboxylate was added into 70 ml ethanol to form solution B. Then, solutions of A and B were mixed and carried into an ultrasonic bath (SK2210HP, KUDOS) at a frequency of 53 KHz for 20 min at room temperature. Finally, the ZnBTC was obtained by vacuum drying after washed with deionized water and ethanol each for 3 times. Finally, ZnBTC nanorods were carbonized in a nitrogen flow with a ramping rate of 5 °C/min and maintained at 900 °C for 3 h.

   Preparation of DC-Cl (Defects engineering carbon with NaCl): 0.45g NaCl and 0.55 g $Zn(CH_3COO)_2{\cdot}2H_2O$ were respectively dispersed in 10 ml aqueous solution to form solution A. 0.525 g of 1,3,5-benzenetricarboxylate was added into 70 ml ethanol to form solution B. Then, solutions of A and B were mixed and carried into an ultrasonic bath (SK2210HP, KUDOS) at a frequency of 53 KHz for 20 min at room temperature. Finally, the ZnBTC+NaCl was obtained by vacuum drying after washed with deionized water and ethanol each for 3 times. Finally, the powder was carbonized in a nitrogen flow with a ramping rate of 5 °C/min and maintained at 900 °C for 3 h.

   Preparation of DC: The DC-Cl was carbonized in a hydrogen flow with a ramping rate of 5 °C/min and maintained at 700 °C for 3 h to remove the Cl atoms in DC-Cl.

2. Electrochemical measurements

The electrochemical tests were carried out in a three-electrode system on an electrochemical workstation (Princeton Applied Research PARSTAT 4000). A glassy carbon (GC) electrode (diameter of 6 mm with surface area of 0.283 cm^2) was used as a working electrode, while platinum foil and Ag/AgCl (3.5 M KCl) electrode were utilized as the counter electrode and reference electrode, respectively. Typically, 4 mg of catalyst and 30 μL of Nafion solution (5 wt%) were dispersed in 1 mL ethanol solution by sonication for 2 h. Then 10 μL of the dispersion was loaded onto a glassy carbon electrode. The prepared electrodes were dried for further use.

The NRR tests were performed electrochemical reduction, the electrochemical measurements we re carried out in a H-cell system which was separated by Nafion 115 membrane. The tests were in N2 saturated 0.1 mol L-1 KOH solution (90 mL) and the electrolyte was stirred and bubbled with N2 gas for 30 min before the tests. All potentials were described versus the reversible hydrogen electrode (RHE) via the following equation: E (vs RHE) = E (vs Ag/AgCl) + 0.21 V + 0.0591 ×pH. Cyclic voltammogram (CV) and linear sweep voltammogram (LSV) were performed at a scan rate of 10 mV s-1 and 5 mV s-1, respectively. All Linear sweep voltammograms (LSV) measurements were steady-state ones after several cycles. The chronoamperometry curves were recorded at different potentials for 2 h.

3. Determination of ammonia

Colorimetric method

The concentration of produced ammonia was determined by Indophenol blue method. 2 mL of reaction solution was added to test tubes. Then, 2 mL of a 1 M NaOH solution containing 5wt% salicylic acid and 5 wt% sodium citrate,1 mL of 0.05 M NaClO and 0.2 mL of an aqueous solution of 1 wt % $C_5FeN_6Na_2O$ (sodium nitroferricyanide) were added in order. ***All solution should prepared freshly when it will be used.*** After mixing up and standing for 1 h, the concentration of the NH_4^+ was measured by UV-vis spectrophotometer(Persee TU-1810).

Cation chromatography method

After NRR test, 10 mL obtained NH_4^+ solution in 0.1 M KOH was adjusted pH to 3 before analysis by cation chromatography (IC 1040, Techcomp). The NH_4^+ peak was observed at 4.5 min. Calibration curve was built to quantify the ammonium ion in the solution.

Calculation of ammonia yield rate and Faradaic efficiency

The Faradaic efficiency for NRR was defined as the amount of electric charge used for synthesizing NH_3 divided by the total charge passed through the electrodes during electrolysis. The total amount of NH_3 produced was measured by colorimetric methods. Assuming three electrons were required to produce one NH3 molecule, the Faradaic efficiency could be calculated as:

$$Faradaic\ efficiency = \frac{3 * F * C_{NH3} * V}{17 * Q}$$

The ammonia yield rate (v_{NH3}) was calculated as:

$$v_{NH3} = \frac{C_{NH3} * V}{t * m_{cat}}$$

where F is the Faraday constant, c_{NH3} is the measured ammonia concentration with

indophenol method, V is the volume of electrolyte for NRR, Q is the quantity of applied electricity, t is the electro-reaction time, and m_{cat} is the mass of loading catalyst.

$^{15}N_2$ isotope labeling experiments

99 at% $^{15}N_2$ (Wuhan Newradar Special Gas Co. Ltd) was used as the feeding gas to perform the isotopic labeling NRR experiment in order to clarify the source of ammonia. The electrochemical reactor was sealed, degassed and filled with Ar for three times, then refilled with $^{15}N_2$ gas. After NRR for 24 h, the obtained solution was concentrated adjusted and identified by ^{1}H NMR spectroscopy (Bruker ASCEND 600 MHz). $^{14}N_2$ experiment was also performed in the same condition for comparison.

4. Materials characterization

The powder X-ray diffraction patterns of the samples were collected on Rigaku D/MAX-γA with Cu-Kα radiation (λ=1.54178 Å) .The morphology of as-prepared samples was observed by field emission scanning electron microscope (FESEM) on a JEOL JSM-6700 M scanning electron microscope. Transmission electron microscopy (TEM) images were performed on a Hitachi H7650 transmission electron microscope with an accelerating voltage of 200 kV. XPS was measured on an ESCALAB 250 X-ray photoelectron spectrometer using Al Kα radiation. The HAADF STEM images were imaged by using a Titan 80-300 scanning/transmission electron microscope operated at 300 kV, equipped with a probe spherical aberration corrector. TGA was carried out using a Shimadzu-50 thermoanalyser under flowing nitrogen atmosphere and with a heating rate of 10℃min-1. XPS was performed on an ESCALAB 250 X-ray photoelectron spectrometer using Al Ka radiation. The specific surface area was evaluated at 77 K (Micromeritics ASAP 2020) using the Brunauer–Emmett–Teller (BET) method applied to the adsorption branch. The data was normalized and analyzed using Athena and Artemis software. The background subtraction and normalization procedures were carried out using standard routines with default parameters determined by the Athena software.

5. DFT caculations

DFT calculations were performed by using the Vienna ab-initio simulation package (VASP). The generalized gradient approximation in the Perdew-Burke-Ernzerhof form was used to describe the exchange and correlation energy. The cutoff energy of plane-wave basis set is 400 eV. As for geometric optimization, the atomic positions were optimized until the forces were less than 0.02 eV/Å and 3× 3 × 1 Monkhorst-Pack sampled k-points were used in all slabs system. In the electronic structure calculations, a larger set of k-points (11×11×1) was used. Accordingly, the ΔG value can be obtained as follows:

$$\Delta G = \Delta E + \Delta ZPE - T\Delta S$$

where ΔE is the electronic energy difference, ΔZPE is the change in zero-point energies, T is the temperature (T = 298.15 K), and ΔS is the change of entropy

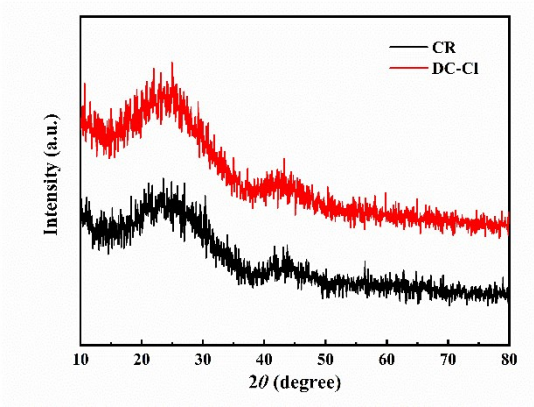

Figure S1. XRD patterns of CR and DC-Cl.

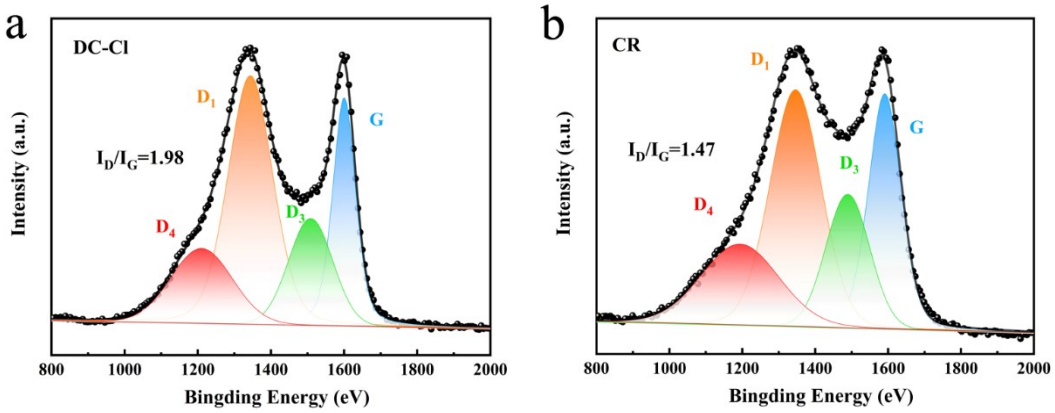

Figure S2. Raman spectra of DC-Cl and CR.

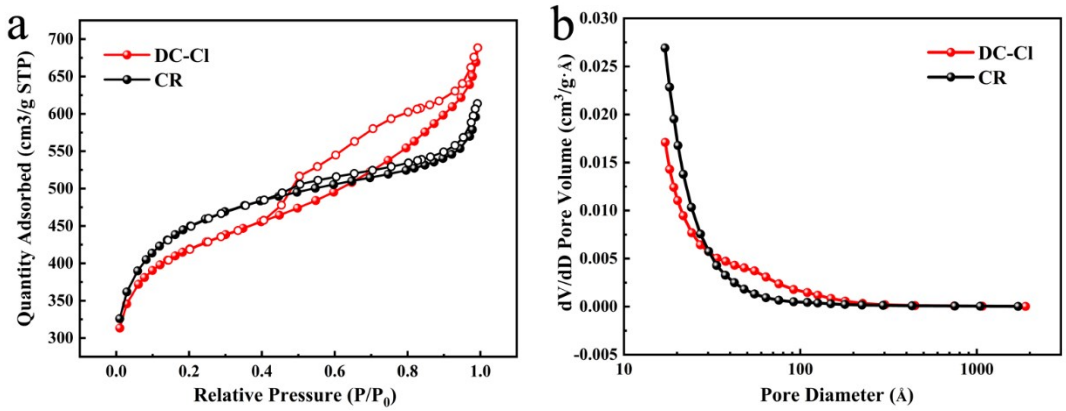

Figure S3 a) Nitrogen adsorption and desorption isotherm and b) pore size distribution curves of CR and DC-Cl.

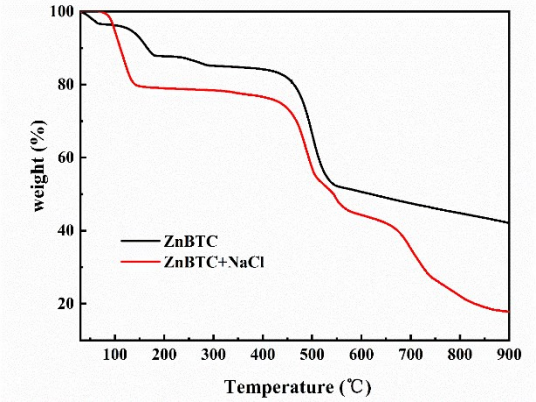

Figure S4 Thermogravimetric analysis (TGA) curves of ZnBTC and ZnBTC+NaCl under nitrogen atmosphere.

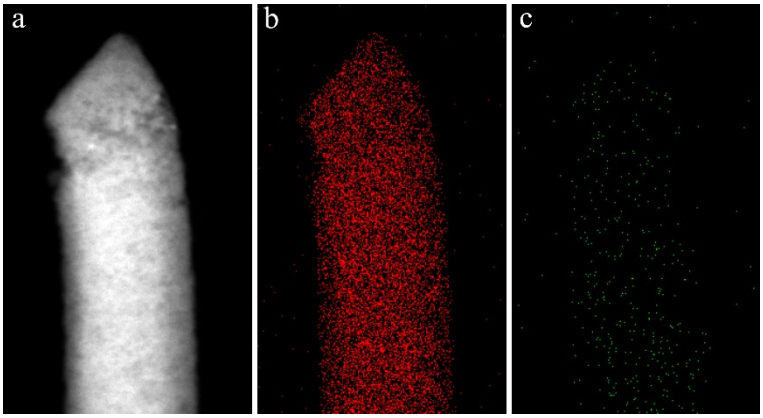

Figure S5. a) HAADF-STEM image of CR. b-c) Images of elemental mapping of C and O respectively.

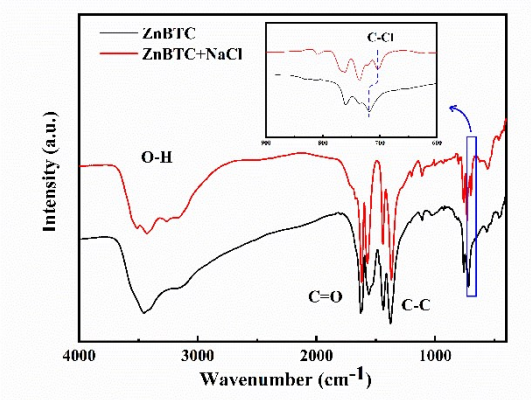

Figure S6. Infrared radiation (IR) spectroscopy of precursors of ZnBTC and ZnBTC+NaCl. ZnBTC+NaCl has a blue shift of 9.16 cm^{-1} than ZnBTC.

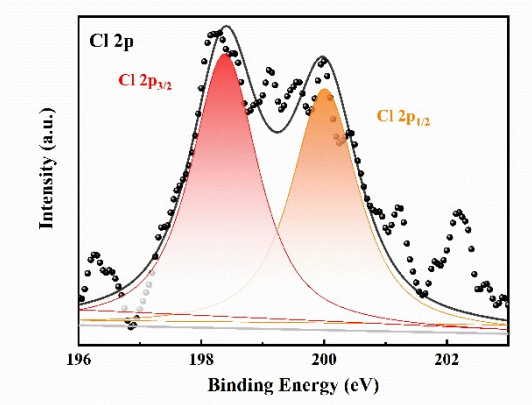

Figure S7. XPS of Cl 2p of DC-Cl.

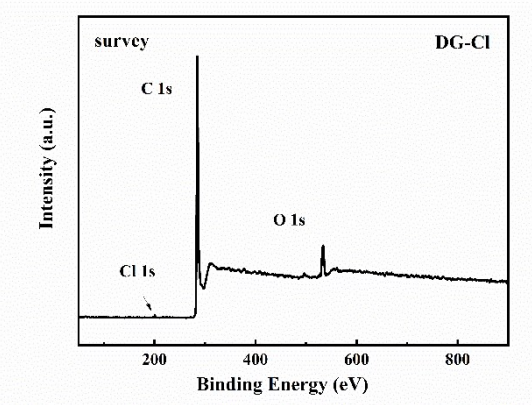

Figure S8. XPS survey of DC-Cl.

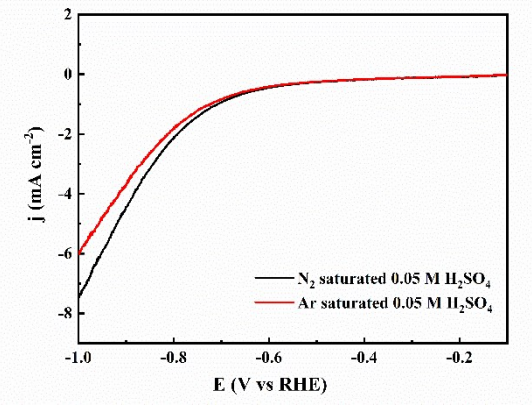

Figure S9. LSV curves survey of DC-Cl in Ar- and N_2- saturated 0.05M H_2SO_4 solution.

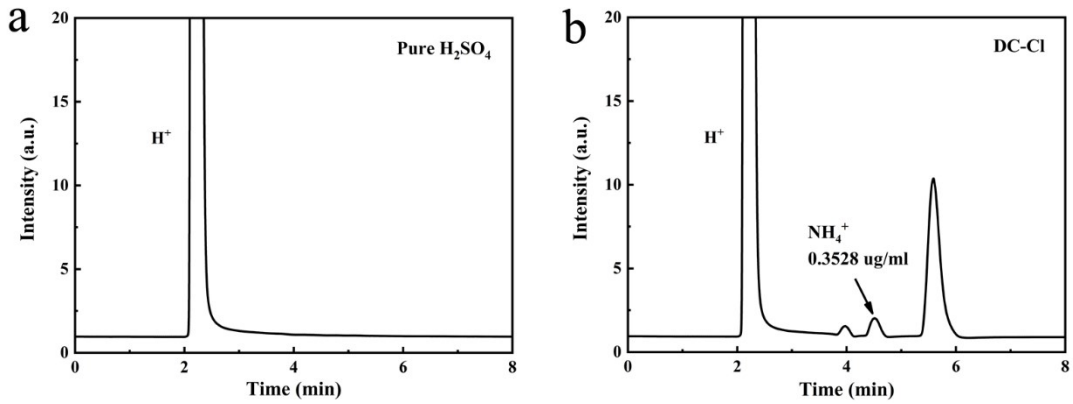

Figure S10. Cation chromatography curves of pure H_2SO_4 and solution of DC-Cl measured at -0.8 V for 2 hours.

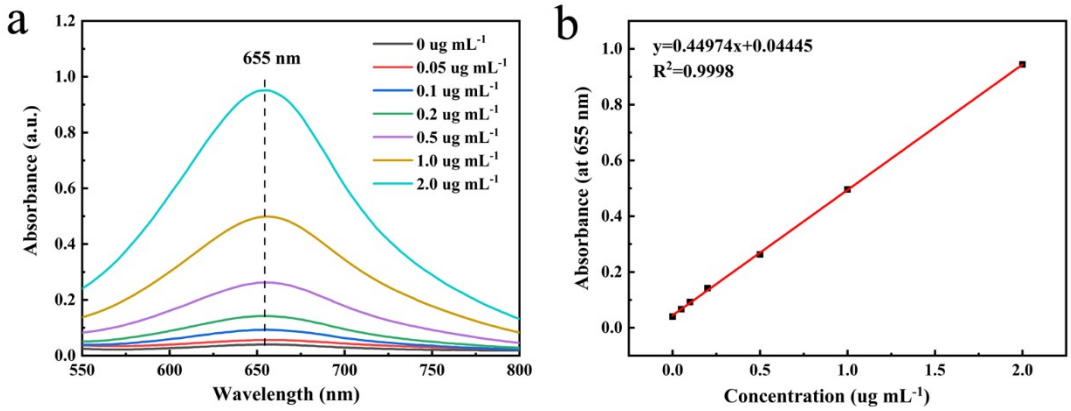

Figure S11. (a) UV-vis curves and (b) concentration-absorbance curve of NH_4^+ ions solution with a series of standard concentrations. The absorbance at 655 nm was measured using a UV-vis spectrophotometer, every points have been texted for three times.

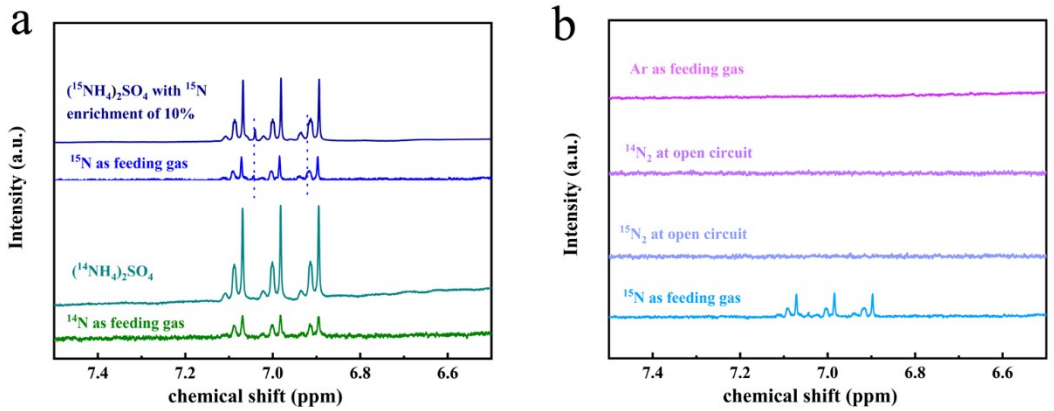

Figure S12. a) ^1H NMR spectra of NH_4^+ and $^{15}NH_4^+$ produced from N_2 electroreduction using N_2 or $^{15}N_2$ as the feeding gas and standard samples. b) ^1H NMR spectra of NH_4^+ and $^{15}NH_4^+$ produce using Ar or $^{15}N_2$ as feeding gas and N_2 or $^{15}N_2$ at open circuit.

For the limitation of expenditure, we have no chance to use $^{15}N_2$ gas for a lot attempts. The impure $^{15}N_2$ gas and imperfect sealed device let in N_2 gas from the air which contribute to NH_4^+ peaks in ^1H NMR. The coupling constant for $^{15}N_2$ is 72.76 and the coupling constant for $^{14}N_2$ is 52.2.We also carried out a series of control text to prove the existence of $^{15}NH_4^+$ in our solution after NRR process.

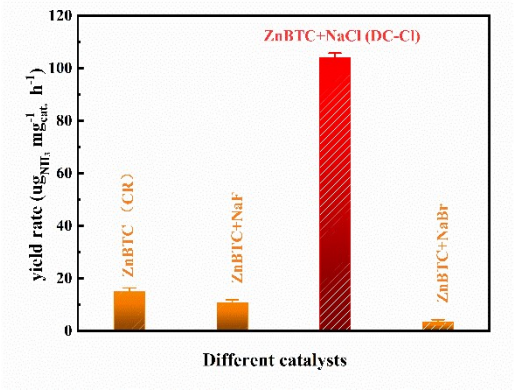

Figure S13. Ammonia yield rate of different catalysts.

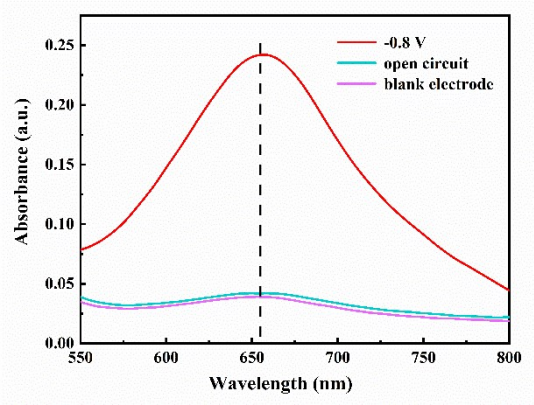

Figure S14. UV-vis curves of DC-Cl with N_2 at -0.8 V, at open circuit potential and blank electrode with N_2 at -0.8 V.

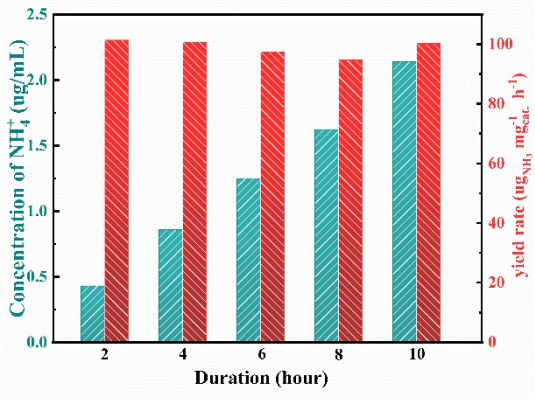

Figure S15. Ammonia concentration and corresponding yield rate for different reaction time.

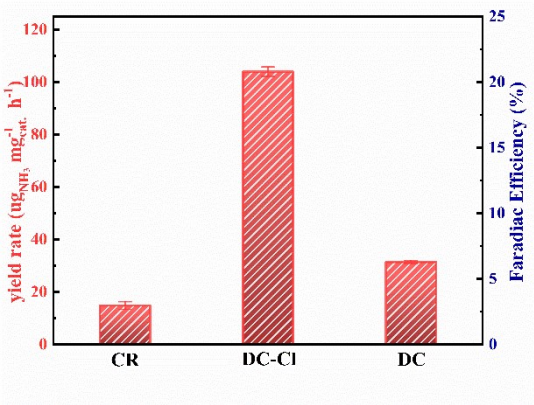

Figure S16. Ammonia yield rate of CR, DC-Cl, DC.

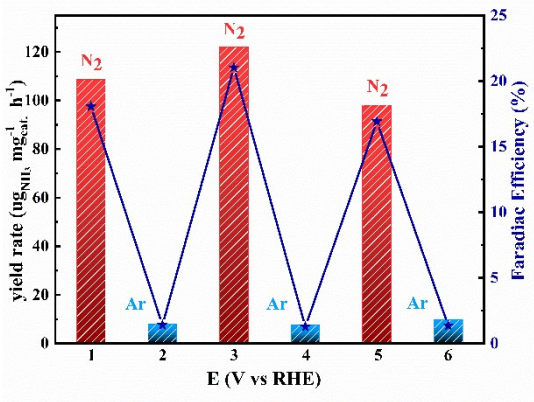

Figure S17. NH_3 yield of N_2 and Ar crossover gas text.

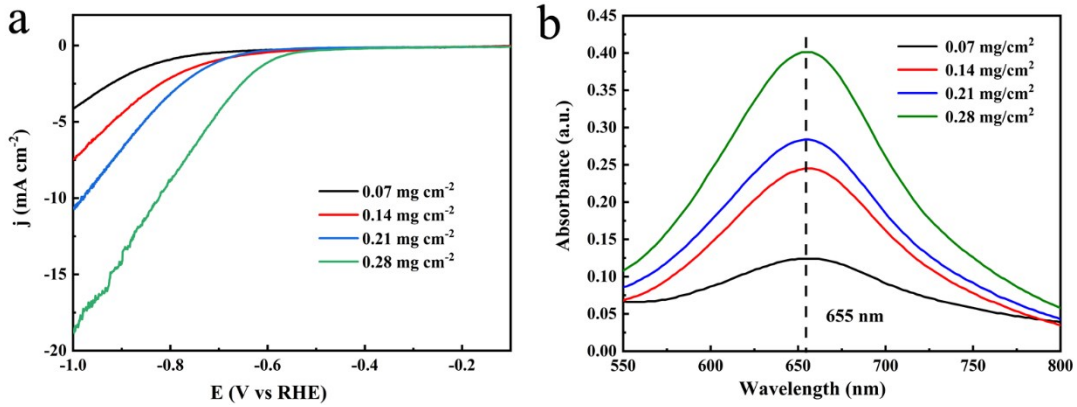

Figure S18. LSV curves and UV-vis curves of DC-Cl with different catalyst loading.

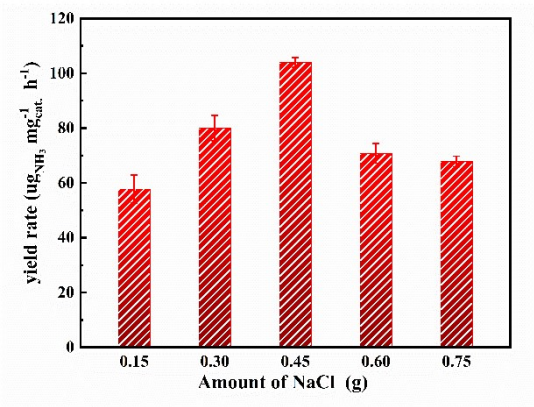

Figure S19. NH_3 yield of DC-Cl with different amount of NaCl adding in the precursor.

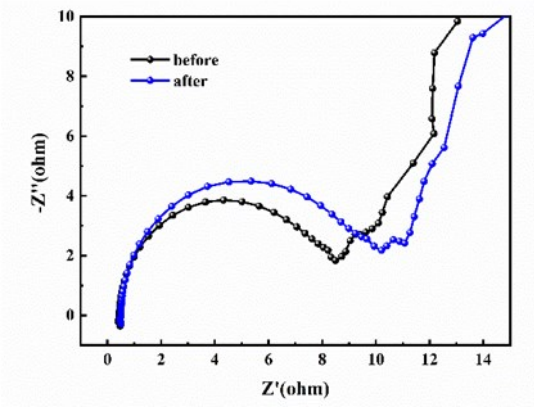

Figure S20. Charge transfer resistance (Rct) of DC-Cl before and after NRR.

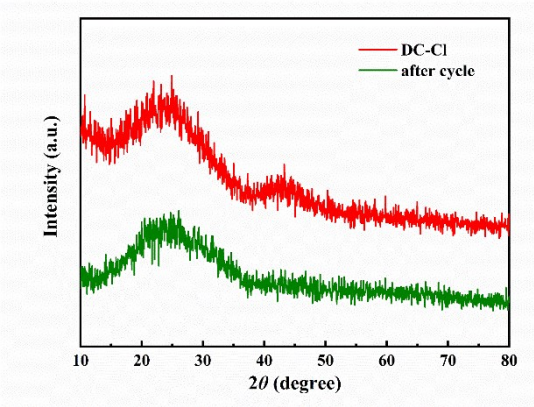

Figure S21. XRD spectra of DC-Cl before and after electrochemical test.

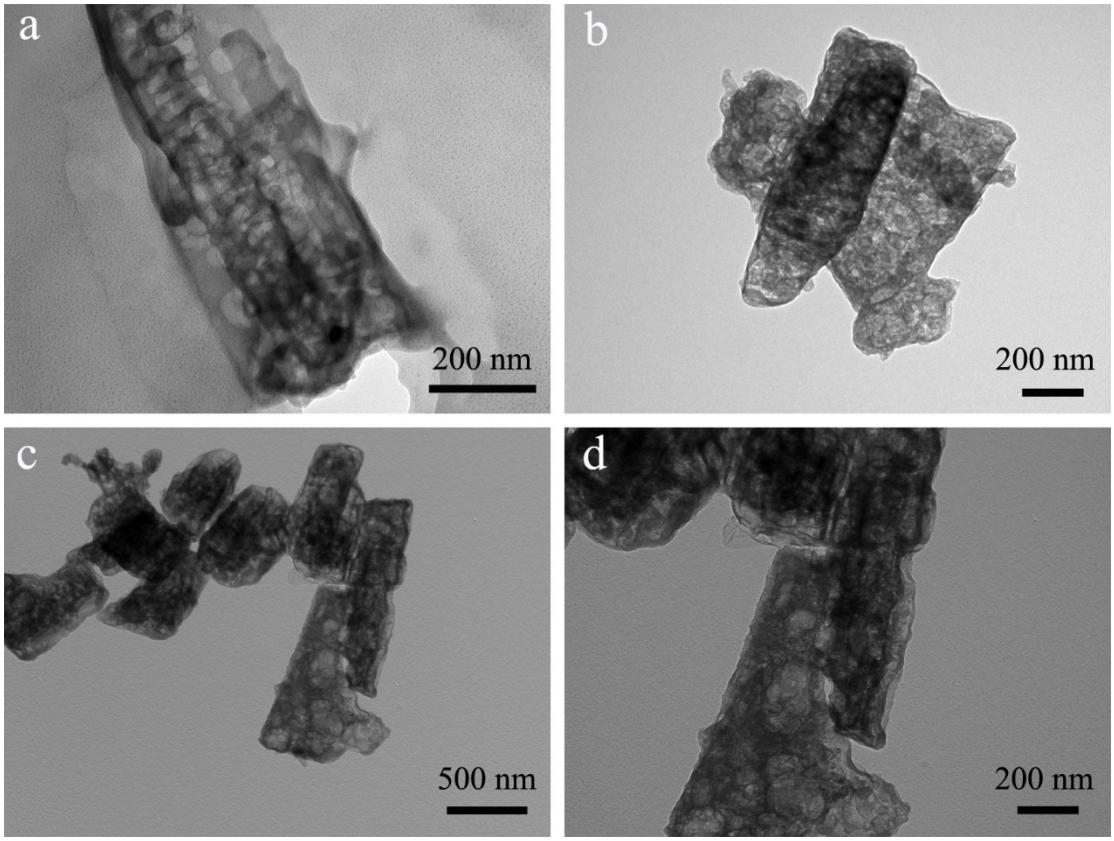

Figure S22. a) and b) TEM pictures of DC-Cl before electrochemical test; c) and d) TEM pictures of DC-Cl after electrochemical test.

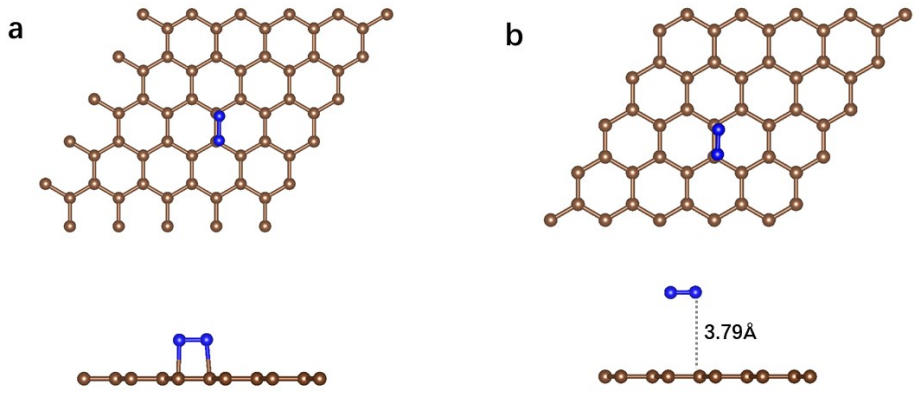

Figure S23. The perfect graphene with adsorbed N_2 molecule a) before structure optimization. b) after structure optimization.

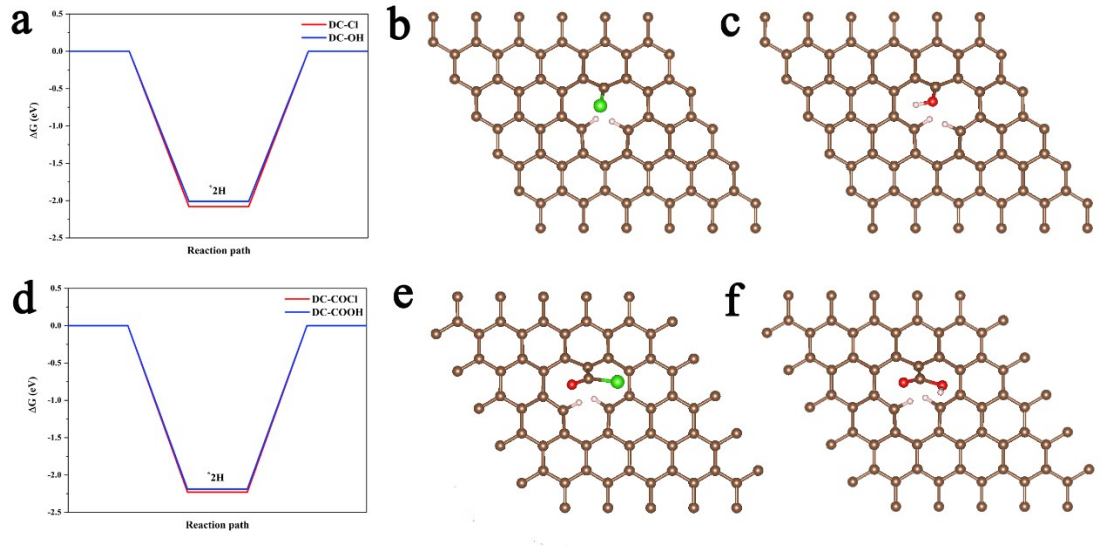

Figure S24. Gibbs free energy diagrams of the H_2 electroreduction for a) DC-Cl and DC-OH d)DC-COCl and DC-COOH. The top-view structure models of intermediates in HER for b) DC-Cl, c) DC-OH, e) DC-COCl, f) DC-COOH.

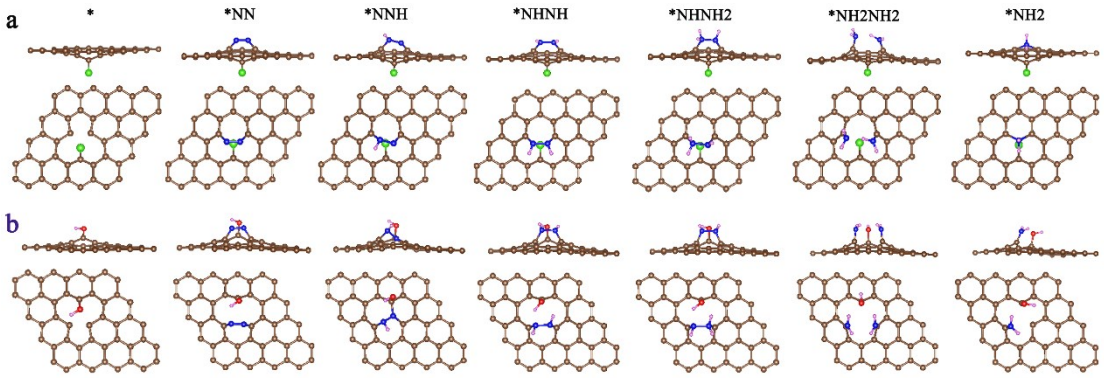

Figure S25. The side-view and top-view structure models of intermediates in NRR for a) DC-Cl. b) DC-OH.

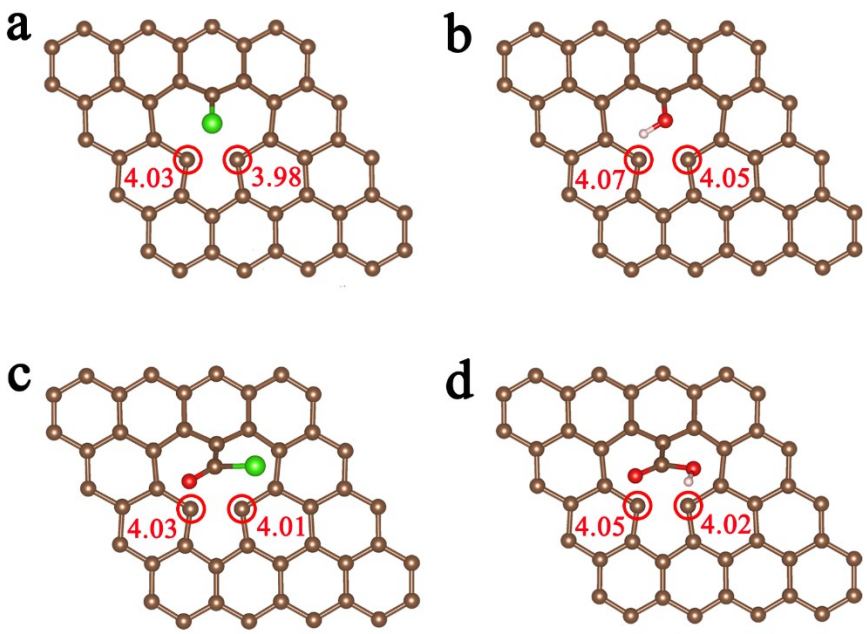

Figure S26. The calculated Bader charges of active carbon atoms for a) DC-Cl, b) DC-OH, c) DC-COCl and d) DC-COOH.

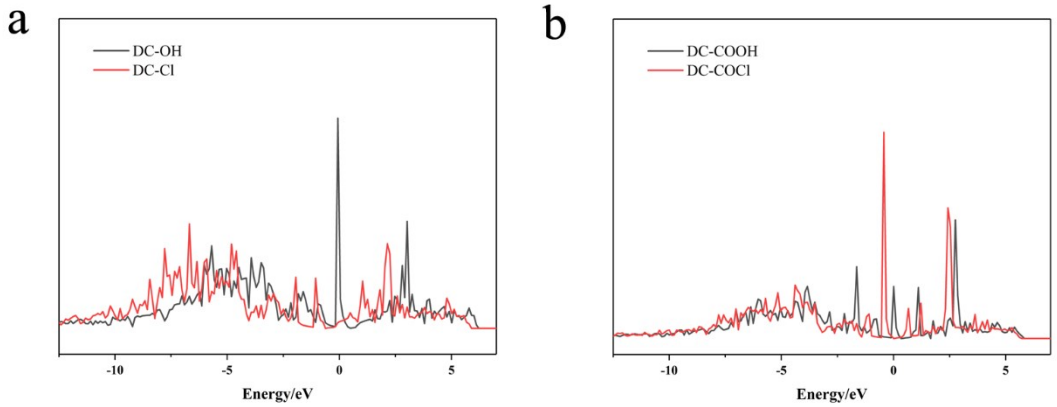

Figure S27. The density of states of active carbon atoms for a) DC-OH and DC-Cl. b) DC-COOH and DC-COCl.

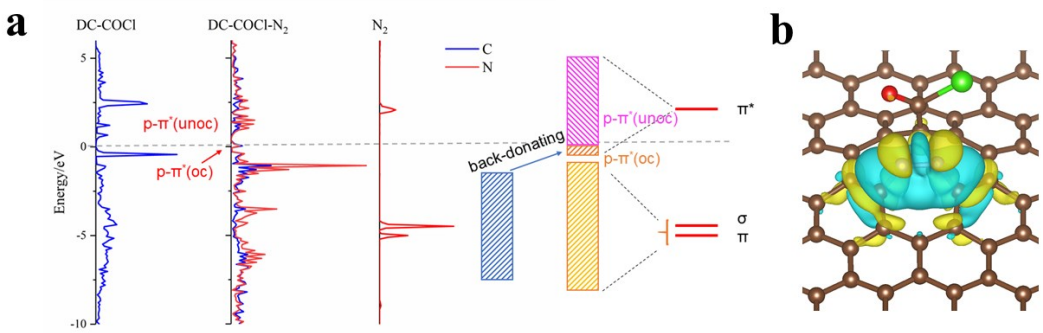

Figure S28. a) Electronic density of states (DOS) and schematic illustrations of p orbitals of DC-COCl, p orbitals of N_2 molecule and their interaction within DC-COCl-N2 configuration. b)

Charge density differences of DC-COCl with the adsorption of N_2.

Samples	BET Surface Area (m^2/g)	Total pore volume（cm^3/g）	Pore diameter（Å）
CR	1,435.0997	0.949505	38.737
DC-Cl	1,396.0997	1.064848	53.296

Table S1. Brunauer–Emmett–Teller (BET) information of CR and DC-Cl.

Different Catalyst Loading	Indophenol blue method	Ion chromatograph method
0.07 mg cm^{-2}	0.1868 ug ml^{-1}	0.2391 ug ml^{-1}
0.14 mg cm^{-2}	0.4155 ug ml^{-1}	0.3528 ug ml^{-1}
0.21 mg cm^{-2}	0.5723 ug ml^{-1}	0.5612 ug ml^{-1}
0.28 mg cm^{-2}	0.6507 ug ml^{-1}	0.6053 ug ml^{-1}

Table S2. Concentration of NH_4^+ (ug/mL) with different catalyst loading by the indophenol blue method and cation chromatograph method.

Material	Electrolyte	Yield(ug h^{-1} mg_{cat}^{-1})	FE	Ref.
DC-Cl	0.05 M H_2SO_4	103.96	21.71%	This work
a-Au/CeOx-RGO	0.1 M HCl	8.3	10.1%	[1]
β-FeOOH	0.5 M $LiClO_4$	23.32	6.7%	[2]
Mo_2N	0.1 M HCl	74.8	4.5%	[3]
Nb_2O_5	0.1 M HCl	43.6	9.26%	[4]
Bi	0.1 M Na_2SO_4	5.453	11.68%	[5]
BP@SnO_{2-x}	0.1 M Na_2SO_4	48.87	14.6%	[6]
W_2N_3	0.1M KOH	11.67	11.66%	[7]
MoS_2	0.1 M Na_2SO_4	29.28	8.34%	[8]
MoS_2-Ru	0.1 M Na_2SO_4	6.98	17.6%	[9]
B_4C	0.1 M HCl	26.57	15.95%	[10]
FC	0.05 M H_2SO_4	6.9	12.1%	[11]
S-NV-C_3N_4	0.5 M $LiClO_4$	32.7	14.1%	[12]

Table S3 Summary of the catalytic performances for some reported NRR electrocatalysts.

1. S. Mukherjee, D. A. Cullen, S. Karakalos, K. Liu, H. Zhang, S. Zhao, H. Xu, K. L. More, G. Wang and G. Wu, *Nano Energy*, 2018, **48**, 217-226.
2. X. Zhu, Z. Liu, Q. Liu, Y. Luo, X. Shi, A. M. Asiri, Y. Wu and X. Sun, *Chem Commun (Camb)*, 2018, **54**, 11332-11335.
3. X. Ren, G. Cui, L. Chen, F. Xie, Q. Wei, Z. Tian and X. Sun, *Chem Commun (Camb)*, 2018, **54**, 8474-8477.
4. F. Lü, S. Zhao, R. Guo, J. He, X. Peng, H. Bao, J. Fu, L. Han, G. Qi, J. Luo, X. Tang and X. Liu, *Nano Energy*, 2019, **61**, 420-427.
5. Y. Wang, M. M. Shi, D. Bao, F. L. Meng, Q. Zhang, Y. T. Zhou, K. H. Liu, Y. Zhang, J. Z. Wang, Z. W. Chen, D. P. Liu, Z. Jiang, M. Luo, L. Gu, Q. H. Zhang, X. Z. Cao, Y. Yao, M. H. Shao, Y. Zhang, X. B. Zhang, J. G. Chen, J. M. Yan and Q. Jiang, *Angew Chem Int Ed Engl*, 2019,

58, 9464-9469.

6. Y. T. Liu, D. Li, J. Yu and B. Ding, *Angew Chem Int Ed Engl*, 2019, **58**, 16439-16444.
7. H. Jin, L. Li, X. Liu, C. Tang, W. Xu, S. Chen, L. Song, Y. Zheng and S. Z. Qiao, *Adv Mater*, 2019, **31**, e1902709.
8. H. Chen, Z. Gu, H. An, C. Chen, J. Chen, R. Cui, S. Chen, W. Chen, X. Chen, X. Chen, Z. Chen, B. Ding, Q. Dong, Q. Fan, T. Fu, D. Hou, Q. Jiang, H. Ke, X. Jiang, G. Liu, S. Li, T. Li, Z. Liu, G. Nie, M. Ovais, D. Pang, N. Qiu, Y. Shen, H. Tian, C. Wang, H. Wang, Z. Wang, H. Xu, J.-F. Xu, X. Yang, S. Zhu, X. Zheng, X. Zhang, Y. Zhao, W. Tan, X. Zhang and Y. Zhao, *Science China Chemistry*, 2018, **61**, 1503-1552.
9. B. Hu, M. Hu, L. Seefeldt and T. L. Liu, *ACS Energy Letters*, 2019, **4**, 1053-1054.
10. W. Qiu, X. Y. Xie, J. Qiu, W. H. Fang, R. Liang, X. Ren, X. Ji, G. Cui, A. M. Asiri, G. Cui, B. Tang and X. Sun, *Nat Commun*, 2018, **9**, 3485.
11. D. Yuan, Z. Wei, P. Han, C. Yang, L. Huang, Z. Gu, Y. Ding, J. Ma and G. Zheng, *Journal of Materials Chemistry A*, 2019, **7**, 16979-16983.
12. K. Chu, Q.-q. Li, Y.-p. Liu, J. Wang and Y.-h. Cheng, *Applied Catalysis B: Environmental*, 2020, **267**.